Tellus SERIES A DYNAMIC METEOROLOGY AND OCEANOGRAPHY
PUBLISHED BY THE INTERNATIONAL METEOROLOGICAL INSTITUTE IN STOCKHOLM

Tellus (2011), 63A, 817–827
Printed in Singapore. All rights reserved

TELLUS

On the meridional structure of extra-tropical Rossby waves

By YOSEF ASHKENAZY[1]*, NATHAN PALDOR[2] and YAIR ZARMI[1], [1]*Solar Energy and Environmental Physics, BIDR, Ben-Gurion University of the Negev, Midreshet Ben-Gurion 84990, Israel;* [2]*Institute of Earth Sciences, The Hebrew University of Jerusalem, Jerusalem 91904, Israel*

(Manuscript received 27 June 2010; in final form 21 January 2011)

ABSTRACT

The common derivation of Rossby waves is based on the quasi-geostrophic approximation. A simple non-harmonic approximation for extratropical Rossby waves on the sphere is proposed, in which the meridional coordinate is a parameter instead of a continuous variable. It is shown that, in contrast to the quasi-geostrophic solution, to first order the meridional structure of these non-harmonic Rossby waves becomes irrelevant for determining the dispersion relation in this theory. The proposed approximation accurately reproduces numerical results obtained from runs of an ocean general circulation model initiated from several initial meridional structures and captures the latitudinal dependence of the phase speed of these waves. The proposed theory yields explicit expressions for the dispersion relation and for the meridional structure of the waves.

1. Introduction

Rossby waves (Rossby, 1939), also known as 'second class' waves (Margules, 1893; Hough, 1898), are usually derived based on the quasi-geostrophic approximation on the β-plane (Rossby, 1939; Gill, 1982; Pedlosky, 1987). Yet, exact solutions for Rossby waves that are based on the linearized shallow water equations and do not employ the quasi-geostrophic approximation have also been derived both on the sphere (e.g. Longuet-Higgins, 1968a; De-Leon and Paldor, 2011) and on the β-plane (e.g. Gill, 1982; Paldor and Sigalov, 2008). These exact solutions are more complicated than the simple (i.e. described by trigoimetric functions) quasi-geostrophic solutions, and have therefore, received less attention.

According to the classical quasi-geostrophic approximation (Rossby, 1939; Gill, 1982; Pedlosky, 1987), Rossby waves are expressed as harmonic (sinusoidal) waves in the zonal and meridional directions where their frequency (and hence the phase speed) is determined by the values of the Coriolis parameters f_0 and β in the middle of the domain. It is thus clear that according to the quasi-geostrophic theory, an initial zonal eigenmode should propagate zonally and uniformly along a latitude circle as long as the conditions for the validity of the quasi-geostrophic approximation are satisfied. However, it is known in the community of ocean general circulation modellers that different meridional sections of a single perturbation propagate with different zonal phase speeds; see further discussion and demonstrations in Section 2 below. This phenomenon is sometimes referred to as 'β-dispersion' (see, Schopf et al., 1981).

The main goal of this study is to present a simple approximation, valid for latitudinal scales of tens of degrees, for extra tropical Rossby waves that accounts for the latitudinal variations in the Rossby wave dispersion relation (or frequency). The proposed approximation provides estimates for the time evolution of an arbitrary initial condition in the meridional direction. For this purpose, we study the linearized shallow water equations (LSWE) on a sphere in a framework where the meridional coordinate is a parameter, allowing a simple derivation of the wave's structure and dispersion relation. The suggested approximations are successfully validated by comparing our analytical estimates to numerical ones obtained from the Massachusetts Institute of Technology general circulation model (MITgcm, Adcroft et al., 2002).

The paper is organized as follows. In Section 2, we show that an initial condition consisting of a single quasi-geostrophic eigenmode in a wide latitudinal range on the β-plane, propagates with different zonal phase speeds in different latitudes although they should have the same phase speed as a function of latitude according to the quasi-geostrophic approximation. We then show that the exact single parabolic cylinder Rossby wave solution does preserve its latitudinal structure with time, and that a linear combination of the exact eigenmodes actually

*Corresponding author.
e-mail: ashkena@bgu.ac.il
DOI: 10.1111/j.1600-0870.2011.00516.x

leads to the classical Rossby wave dispersion relation. A new approximation for the extra-tropical Rossby waves is suggested in Section 3. Numerical simulations obtained by the MITgcm are then compared to the analytical approximation in Section 4. A summary and discussion then follow (Section 5).

2. Rossby waves in a mid latitude channel: quasi-geostrophic approximation versus numerical simulations

We use the MITgcm (Marshall et al., 1997a,b; Adcroft et al., 2002) for the numerical simulations. The MITgcm is a free surface, finite volume, z-coordinate model with shaved/partial bottom cells. Various state-of-the-art subgrid parametrizations and boundary layer schemes may be used in this model. In the past, the model has been used in the study of systems over a wide range of temporal and spatial scales (from scales of several degrees down to a few metres) (Adcroft et al., 2002).

Here we study the dynamics of Rossby waves in a channel with flat bottom on the β-plane and on a sphere. The numerical configuration was chosen as follows: one vertical layer of depth $H = 500$ m over 360° in the zonal direction and various distributions (described below) in the meridional direction. The gravitation constant in all simulations is $g = 0.01$ m s^{-2}, so that with the channel depth of H the gravity wave speed is $\sqrt{gH} \approx 2.2$ m s^{-1}, a typical value for baroclinic phase speeds. Periodic boundary conditions are assumed in the zonal direction and free slip on the channel walls and at the bottom; the meridional velocity is zero at the channel walls. The water density is constant. The implicit free surface scheme of MITgcm was used in the simulations. The numerical simulations include advection and viscosity terms. The integration time step is 1 h. The horizontal viscosity coefficient is 300 m^2 s^{-1} although we used other values to check the sensitivity of the results to the value of this parameter.

To study the characteristics of the first baroclinic mode of planetary Rossby waves, we numerically solve the primitive equations on the β-plane. We consider a channel extending from 20°N to 50°N. The resolution is 1° × 0.5° for the zonal and meridional directions, respectively.

The simulation is initiated with a spatially periodic sea surface height and velocities, with two sinusoidal cycles in the zonal direction and half a sinusoidal cycle in the meridional direction (Fig. 1a). The initial distribution of the velocity components and sea surface height are related to each other in such a way that they comprise an eigenmode of the quasi-geostrophic Rossby wave theory. As can be immediately seen in the free surface height plots of Fig. 1b, after 20 yr of simulation the wave propagates

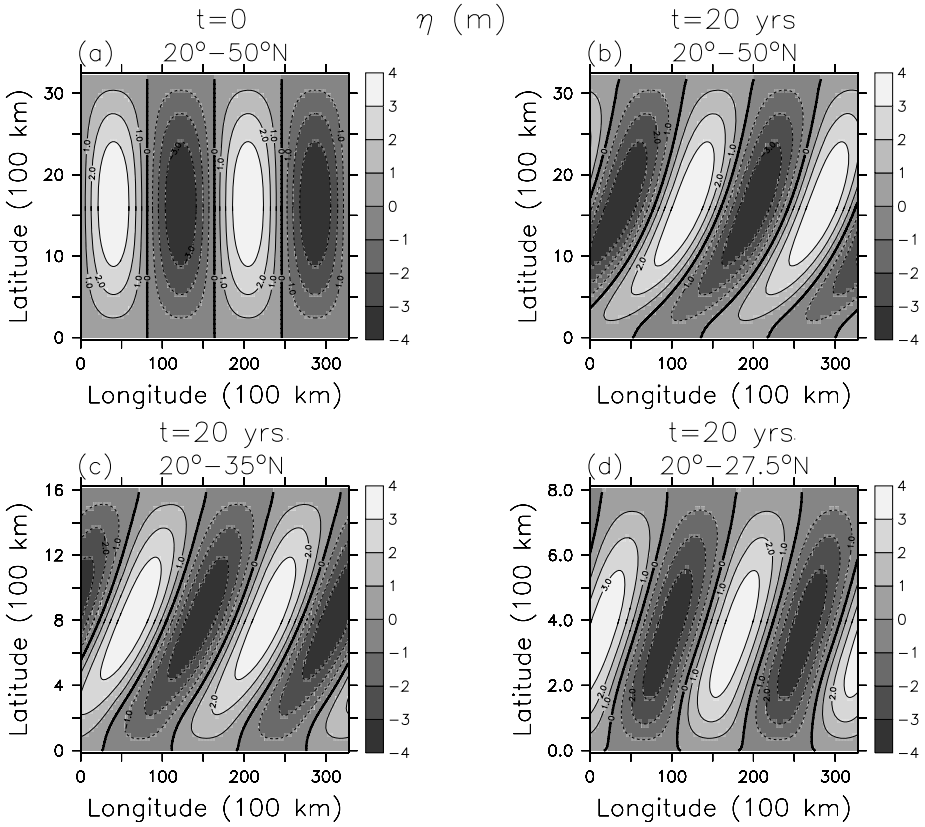

Fig. 1. (a) The initial conditions of the free surface η. (b) The free surface after 20 yr of simulations. Note the greater zonal phase speed towards lower latitudes. (c) Same as b for channel extending from 20° to 35°N. (d) Same as b for channel extending from 20° to 27.5°N.

westward, much farther at low latitudes than at high latitudes. The zonal and meridional velocities exhibit similar latitudinal dependence.

The westward propagation of the wave, the main property that characterizes Rossby waves, is evident from Fig. 1. Moreover, the analysed phase speed for each latitude (not shown) coincides with the well known long Rossby wave phase speed (e.g. Pedlosky, 1987) at latitude $f_0 + \beta y$

$$C_x(y) \approx -\frac{\beta g H}{(f_0 + \beta y)^2}, \tag{1}$$

where f_0 and β are the β-plane parameters; eq. (1) may be obtained by replacing f_0 with $f_0 + \beta y$ in the known phase speed $C_x(y) = -\beta g H / f_0^2$. However, according to the quasi-geostrophic approximation, the wave should have propagated uniformly with latitude with a phase speed corresponding to the middle of the channel. The difference in the zonal phase speed between the northern part of the channel and the southern part is large and significant.

We repeated the above experiment for different channel widths, corresponding to meridional extents of 20°N to 35°N (Fig. 1c) and 20°N to 27.5°N (Fig. 1d); the meridional resolution is 0.25° and 0.125°, respectively. For both cases the wave propagation is largely dependent on latitude. The quasi-geostrophic approximation is more accurate for channels located further poleward. We use a sufficiently small viscosity coefficient to avoid a smearing effect in the meridional direction, which may lead to seemingly uniform propagation of the wave. Thus, under the typical parameter values we use here, the quasi geostrophic wave theory fails to estimate correctly the phase speed and meridional structure even in a narrow channel that is only 7.5° wide (where the β-plane should apply).

In an alternate theory of the quasi-geostrophic theory, Rossby waves on the β-plane in a channel are derived, by assuming that the solutions can be expressed as the product of a travelling wave solution in the zonal direction and an unknown meridional structure function that satisfies the boundary conditions at the walls. Then, an ordinary differential equation is obtained for the meridional velocity as a function of the meridional coordinate, y. The general solution for this differential equation is the parabolic cylinder function (e.g. Gill, 1982; Paldor and Sigalov, 2008; Poulin, 2009). The parabolic cylinder functions have an oscillatory region equatorward of, and exponentially decaying (or growing) region poleward of, a certain latitude called the turning latitude. The wave frequency, and hence the dispersion relation, is determined by the boundary conditions. The first four eigenmodes of this general parabolic cylinder function solution (numbered '0' to '3') are depicted in Fig. 2a; as the mode number increases, the decay occurs at higher latitudes and more oscillations occur at lower latitudes (the number of extremal points is equal to the mode number plus one). For sufficiently large mode numbers the oscillations extend to the northern wall of the channel.

We next check whether the latitudinal dependence observed for the quasi-geostrophic conditions exists also in the exact solution of Rossby waves on the β-plane. For this purpose we ran the same simulation as in Fig. 1 but now starting with the parabolic cylinder function eigenmodes for the meridional velocity instead of the sinusoidal functions; the initial free surface height and the zonal velocity are calculated from the initial meridional velocity so the combined field is an eigenmode of shallow water system. The initial state and the wave pattern after 20 yr of simulations are presented in Fig. 3; here we use as an example mode '3' and a linear combination of the first four parabolic cylinder modes. While the structure of mode '3' remained almost unchanged throughout the entire 20 yr of westward propagation, the initial linear combination of the first four modes yielded a faster zonal wave speed near the equatorward wall. These numerical simulations validate numerically the correctness of the exact parabolic cylinder function solution.

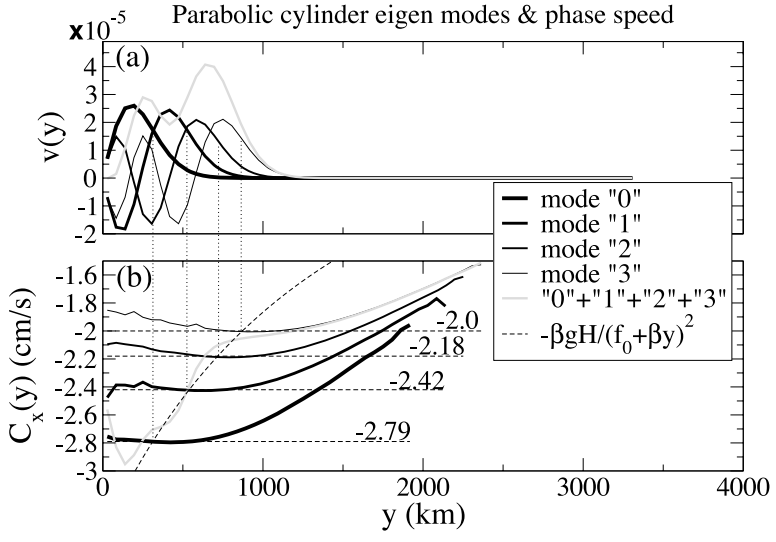

Fig. 2. (a) The first four parabolic cylinder modes (numbered '0' to '3') and their linear combination. (b) The zonal phase speed calculated numerically based on the MITgcm simulations starting from the $v(y)$ as depicted in panel (a). The parabolic cylinder modes exhibit almost uniform phase speed with latitude. However, the linear combination of the first four modes follows the classical long Rossby waves dispersion relation (dashed curve). The vertical dotted lines indicate the point at which the classical Rossby waves phase speed coincides with the parabolic cylinder eigenmodes phase speed. The horizontal dashed lines indicate the theoretical parabolic cylinder eigenmodes phase speeds.

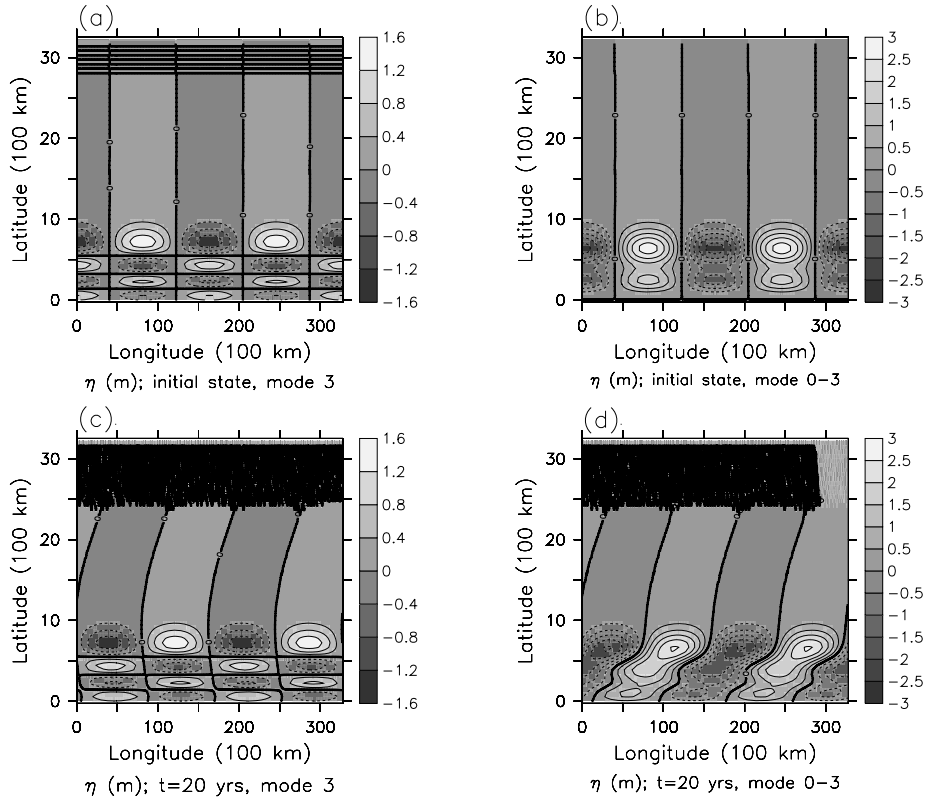

Fig. 3. The initial free surface η (upper panels) for the fourth mode (number '3', left-hand panels) and for the linear combination of the first four modes (right-hand panels). The free surface after 20 yr of simulations is depicted in the lower panels. While mode '3' preserved its structure with time, the linear combination exhibited faster wave propagation towards the south.

We numerically calculate the zonal phase speed as a function of latitude for each of the first four parabolic cylinder eigenmodes and of their linear combination. The results are depicted in Fig. 2b. Also included are the theoretical phase speeds of the modes (horizontal dashed lines) and the classical long Rossby wave zonal phase speed [eq. (1), heavy dotted line]. The zonal phase speed is almost constant over the region where the wave is practically non-zero and in this region it coincides with the theoretical parabolic cylinder phase speed.

The initial state of the linear combination of the first four parabolic cylinder modes propagated with latitude-dependent different zonal phase speed (Figs 2 and 3), similar to the simulation of quasi-geostrophic eigenmode initial conditions depicted in Fig. 1. Moreover, the numerically calculated phase speed follows the classical zonal phase speed [eq. (1)]. It is fairly easy to understand qualitatively the dependence of the phase speed on latitude: since higher parabolic cylinder modes reach higher latitudes they propagate more slowly according to eq. (1). However, the quantitative agreement with eq. (1) is more difficult to understand; see a similar observation in fig. 12.3 of Gill (1982), obtained for the discrete equatorial modes.

The vertical dotted lines in Fig. 2 indicate the crossing points between the parabolic cylinder modes phase speeds and the corresponding long Rossby waves phase speeds [eq. (1)]. These crossing points are the turning latitudes defined above. Our numerical simulations suggest that (i) the exact Rossby wave phase speed follows very closely the classical zonal phase speed [eq. (1)] and that (ii) the turning latitude that separates the oscillatory and exponentially decaying regions of the parabolic cylinder eigenmode characterizes the eigenmode.

It is not straightforward to calculate numerically the eigenvalues of the parabolic cylinder eigenmodes that have no analytical expression. Moreover, when considering the more complete problem of Rossby waves on the sphere, the exact solution is even more complicated as it is expressed as an infinite sum of complicated eigenfunctions (Longuet-Higgins, 1968a). The approximation suggested below aims at providing a simple approximation for Rossby waves on the sphere as well as on the β-plane.

3. A new approximation for Rossby waves on the sphere

There is an infinite number of vertical modes of density stratification in the ocean (Gill, 1982). It is known that each vertical mode can be represented in the LSWE by the appropriate reduced

gravity g and equivalent depth h parameters (e.g. LeBlond and Mysak, 1978); since the first baroclinic mode is the dominant one (Chelton et al., 1998) we choose below parameter values associated with this mode.

For a flat channel of depth H on a sphere the LSWE are (Gill, 1982):

$$\begin{aligned} \frac{\partial u}{\partial t} - 2\Omega \sin\phi v &= -\frac{g}{a\cos\phi}\frac{\partial \eta}{\partial \lambda} \\ \frac{\partial v}{\partial t} + 2\Omega \sin\phi u &= -\frac{g}{a}\frac{\partial \eta}{\partial \phi} \\ \frac{\partial \eta}{\partial t} + \frac{H}{a\cos\phi}\frac{\partial u}{\partial \lambda} + \frac{H}{a}\frac{\partial v}{\partial \phi} - \frac{H}{a}v\tan\phi &= 0, \end{aligned} \tag{2}$$

where λ, ϕ and t are the longitude, latitude and time independent variables, u and v are the zonal and meridional velocities, η is the free surface height, g is the (reduced) gravity constant, a is Earth's radius, and Ω is Earth's angular frequency. Here we neglect the non-linear advection terms since they are very small due to the small velocities (small Rossby number) and ditto the viscosity terms.

Equations (2) may be reduced to a single equation in η following a procedure similar to that given in Pedlosky (2003). First, it is necessary to express the velocities, u, v in terms of η as follows:

$$\begin{aligned} \Re u &= -\frac{g}{a}\left(\frac{1}{\cos\phi}\partial_{t\lambda} + f\partial_{\phi}\right)\eta \\ \Re v &= \frac{g}{a}\left(\frac{f}{\cos\phi}\partial_{\lambda} - \partial_{t\phi}\right)\eta, \end{aligned} \tag{3}$$

where the operator $\Re$ is

$$\Re = \partial_{tt} + f^2, \tag{4}$$

where $f = 2\Omega\sin\phi$ is the Coriolis parameter. After a few algebraic operations a partial differential equation for η is obtained by substituting the expressions for u and v into the third equation of system 2:

$$\left\{\cos\phi\partial_t\Re^2 - \frac{gH}{a^2}\left[2\Omega\cos\phi f^2\partial_{\lambda} + \Re\frac{1}{\cos\phi}\partial_{\lambda\lambda t} - 4\Omega\cos^2\phi f\partial_{t\phi} + \cos\phi\partial_{tt\lambda} + \Re\partial_{\phi}(\cos\phi\partial_{t\phi})\right]\right\}\eta = 0. \tag{5}$$

Equation (5) can be non-dimensionalized using the dimensionless parameter ε

$$\varepsilon = \frac{gH}{(2\Omega a)^2} \tag{6}$$

and by scaling t and λ using this parameter: $\lambda = \sqrt{\varepsilon}\hat{\lambda}$ and $t = \hat{t}/(2\Omega\sqrt{\varepsilon})$ where the 'hat' symbol denotes dimensionless variables. The resulting equation is

$$\left\{\cos\phi\left(\partial_{\hat{t}}\hat{\Re}^2 - \sin^2\phi\partial_{\hat{\lambda}}\right) - \hat{\Re}\frac{1}{\cos\phi}\partial_{\hat{\lambda}\hat{\lambda}\hat{t}} + \varepsilon\left[2\cos^2\phi\sin\phi\partial_{\hat{t}\phi} + \cos\phi\partial_{\hat{t}\hat{t}\hat{\lambda}} - \hat{\Re}\partial_{\phi}(\cos\phi\partial_{\hat{t}\phi})\right]\right\}\eta = 0, \tag{7}$$

where

$$\hat{\Re} = \varepsilon\partial_{\hat{t}\hat{t}} + \sin^2\phi. \tag{8}$$

The boundary conditions of zero meridional velocity at the channel walls may be expressed using eq. (3)

$$-\frac{1}{2\Omega}\partial_{t\phi}\eta + \tan\phi\partial_{\lambda}\eta = 0. \tag{9}$$

(Note that the non-dimensional boundary conditions associated with this dimensional condition only requires the substitution of ε for $1/2\Omega$). Also note that only λ and t are rescaled while ϕ retains its original scale as the latitude angle; η may be rescaled using an arbitrary constant such as H. In addition, note that ε is the inverse of the non-dimensional parameter used in some earlier studies (Longuet-Higgins, 1968a; Margules, 1893; Hough, 1898). A similar scaling applies also on the β-plane provided the LSWE is scaled by: $\hat{t} = t/\beta R$, $\hat{x} = Rx$, $\hat{y} = f_0 y/\beta$, where $R = \sqrt{gh}/f_0$ and in this case the small parameter is $\varepsilon = (\beta R/f_0)^2$. For typical values used in our numerical simulations we obtain $\varepsilon \approx 5.8 \times 10^{-6} \ll 1$. In the scaling presented above, the dimensional time variable is multiplied by $2\Omega\sqrt{\varepsilon}$ to yield the non-dimensional time variable, that is, time is squeezed; this is so since Rossby waves are slow compared to the Earth's rotation. In addition, the original zonal coordinate λ is divided by $\sqrt{\varepsilon}$, meaning 'zonal stretching'. This scaling is motivated by the realization (and the numerical results presented below) that Rossby waves propagate almost entirely in the zonal direction, indicating much faster wave propagation in the zonal direction; this zonal stretching aims at 'slowing' this propagation. In practice the above scaling is equivalent to the assumption of long (or large scale) meridional waves (or perturbations).

The free surface η may be expanded in power of ε

$$\eta = \eta_0 + \varepsilon\eta_1 + \varepsilon^2\eta_2 + \cdots \tag{10}$$

Equation (7) then reduces to a simple equation for the zero-order approximation of the free surface, η_0

$$\left[\partial_{\hat{t}} - \frac{1}{\sin^2\phi}\partial_{\hat{\lambda}}\left(\frac{1}{\cos^2\phi}\partial_{\hat{t}\hat{\lambda}} + 1\right)\right]\eta_0 = 0. \tag{11}$$

Equation (11) does not contain derivatives with respect to the meridional variable ϕ and thus ϕ becomes a mere parameter. This fact yields a simple solution (shown below) that includes the meridional dependence of the wave frequency.

Assuming a wave solution of the form $\eta_0 = \exp[\mathrm{i}(\hat{k}\hat{\lambda} - \hat{\omega}\hat{t} + \delta)]\bar{\eta}_0(\phi) = \exp(\mathrm{i}\theta)\bar{\eta}_0(\phi)$, one obtains the dispersion relation:

$$\hat{\omega}(\phi) = -\frac{\hat{k}_{\lambda}\cos^2\phi}{\sin^2\phi\cos^2\phi + \hat{k}_{\lambda}^2}, \tag{12}$$

where the function $\bar{\eta}_0(\phi)$ may be any smooth function that satisfies the boundary conditions. The corresponding dimensional dispersion relation is

$$\omega(\phi) = -\frac{2\Omega\varepsilon k \cos^2\phi}{\sin^2\phi\cos^2\phi + \varepsilon k_\lambda^2}. \tag{13}$$

The derived dispersion relation and free surface were obtained for the extra-tropics since in the operator $\Re$ the Coriolis parameter is assumed to be much larger than the time derivatives (and hence the Rossby wave frequency), as for the extra-tropics.

At this stage, the zero-order solution is known, since the free surface is the only variable in eq. (7), which is the equivalent equation to the LSWE. Once η_0 is found, it is possible to use it in eq. (3) to obtain two uncoupled ordinary differential equations for the velocities, u and v, where each of these equations is in essence a forced harmonic oscillator equation. Alternatively, it is possible to apply the above scaling in eq. (3) to obtain

$$\begin{aligned}\hat{\Re}\hat{u} &= -\left(\frac{1}{\cos\phi}\partial_{\hat{t}\hat{\lambda}} + \sin\phi\partial_\phi\right)\hat{\eta}\\ \hat{\Re}\hat{v} &= (\tan\phi\partial_{\hat{\lambda}} - \varepsilon\partial_{\hat{t}\phi})\hat{\eta},\end{aligned} \tag{14}$$

where the implied scaling for η, u and v is

$$\eta = H\hat{\eta}, \quad u = 2\Omega a\varepsilon\hat{u}, \quad v = 2\Omega a\sqrt{\varepsilon}\hat{v}. \tag{15}$$

Thus, to the zeroth order in ε the non-dimensional velocities are

$$\hat{u}_0 = \frac{1}{\sin\phi}\left(\hat{t}\cos\theta\hat{\bar{\eta}}_0\hat{\omega}' - \sin\theta\hat{\bar{\eta}}_0' - \frac{\hat{\omega}\hat{k}_\lambda\sin\theta\hat{\bar{\eta}}_0}{\sin\phi\cos\phi}\right), \tag{16}$$

$$\hat{v}_0 = \frac{1}{\sin\phi}\frac{\hat{k}_\lambda\cos\theta\hat{\bar{\eta}}_0}{\cos\phi}. \tag{17}$$

The corresponding zero-order dimensional velocities are then:

$$u_0 = \frac{g}{af}\left(t\cos\theta\bar{\eta}_0\omega' - \sin\theta\bar{\eta}_0' - \frac{\omega k\sin\theta\bar{\eta}_0}{f\cos\phi}\right), \tag{18}$$

$$v_0 = \frac{g}{af}\frac{k\cos\theta\bar{\eta}_0}{\cos\phi}. \tag{19}$$

For long waves ($k \ll 1$), the last term in eq. (18) may be neglected. This case may be associated with the planetary geostrophy solution. It follows from eq. (17) that the boundary conditions $v_0 = 0$ at the channel walls are satisfied only for vanishing free surface η_0 there. Note that u_0 does not have to vanish at the channel wall even if η_0 does, since it includes, according to eq. (18), the derivative of $\bar{\eta}_0(\phi)$.

u_0 contains a secular term, $\omega' t$, and thus it is not bounded at long times. However, the total energy of the system is conserved (Longuet-Higgins, 1968b; Vallis, 2006), such that

$$\frac{\mathrm{d}}{\mathrm{d}t}\int\int(\varepsilon u^2 + v^2 + \eta^2)\cos\phi\,\mathrm{d}\lambda\mathrm{d}\phi = 0. \tag{20}$$

The assumptions that lead to eq. (20) are the standard boundary conditions of vanishing meridional velocity at channel walls and periodic boundary conditions in the zonal direction. Thus, secular terms cannot exist in the exact solution of eqs (3) and (7). The total energy for each order of approximation must be conserved independently of the higher orders. For example, in the zeroth order, the energy of the system is $E_0 = \int\int(v_0^2 + \eta_0^2)\cos\phi\,\mathrm{d}\lambda\,\mathrm{d}\phi$, and is independent of time since v_0 and η_0 are simple harmonic (sinusoidal) functions. In Appendix A, we show that energy is conserved in the first order as well. While secular terms exist in the zero-order zonal velocity, they appear only in the first-order approximation for the free surface and meridional velocity (Appendix A). The secular term in u_0 limits the validity of the approximated u_0 to times that satisfy $\omega' t < 1$ [see eq. (18)] while v_0 and η_0 are valid for longer times. Thus, for high latitudes where ω' is small, the approximation is valid for long times while for low latitudes the approximation is valid for shorter times. Since the frequency ω depends on the wave number, for larger wave numbers (shorter wave lengths) the validity holds for shorter times. For very long waves and for the parameter values used in the numerical simulation described below, the approximation is valid for tens of years while for short waves it is valid only for times of the order of (or even shorter than) a few years.

The dimensional zonal phase speed (in units of length over time) is obtained by multiplying ω/k by $a\cos\phi$

$$C(\phi) = -\frac{gHa\cos\phi}{2\Omega a^2\sin^2\phi + gHk^2/(2\Omega\cos^2\phi)}. \tag{21}$$

For long planetary waves, k is very small, so the second term in the denominator is much smaller than the first term. Thus the phase speed may be approximated by

$$C(\phi) \approx -\frac{gH\cos\phi}{2\Omega a\sin^2\phi}. \tag{22}$$

The zonal periodic boundary conditions impose a trivial quantization condition on the zonal wavenumber, k = integer.

The range of latitudes, for which the approximation is valid, depends on the choice of parameter values. For the simulations presented below, this range is $|\phi| \gtrsim 20^\circ$.

4. Numerical simulations versus analytical approximation

We use, again, the MITgcm to verify the accuracy of the above suggested approximation. We use similar settings as described in Section 2, with the following differences: (i) simulation on the sphere instead on the β-plane, (ii) channel extension from 80°S to 80°N and (iii) grid resolution of 1° in both lateral directions. We refrain from extending the channel up to the poles to avoid numerical complications. The simulation is initiated with a spatially periodic sea surface height, with ten sinusoidal cycles in the zonal direction (i.e. a zonal wave length of 36°), half a sinusoidal cycle in the meridional direction between 60°S to 20°S and a full cycle between 20°N to 60°N; the initial free surface is a multiplication of these functions with an amplitude of $A = 4$ m. Mathematically, the initial free surface is $\eta(t = 0) = 4\sin(10\lambda)\bar{\eta}(\phi)$

where $\bar{\eta}(\phi) = \sin[4.5(\phi - \phi_0)\pi/180]$ for $\phi = 60^\circ$S to 20°S and $\phi_0 = 60^\circ$S and $\bar{\eta}(\phi) = \sin[9(\phi - \phi_0)\pi/180]$ for $\phi = 20^\circ$N to 60°N and $\phi_0 = 20^\circ$N; the free surface is zero otherwise. The same $\bar{\eta}(\phi)$ was used to plot the analytical zero-order approximations given in eqs (18) and (19). The initial velocities are set to zero. We choose the initial state to be far from the channel walls to demonstrate that even for internal perturbation and basically arbitrary meridional structure the suggested approximation is valid; other perturbations extending to the channel walls yielded similar agreement between the numerical results and analytical approximations. We exclude the equatorial region from the initial state since the approximation in its present form is invalid there.

A comparison between the numerical simulations and the approximation, after 15 yr of simulations, is shown in Fig. 4. The initial state has propagated to the west where the equatorward parts propagated much faster than the poleward parts. The agreement between the analytical estimates and numerical calculations is good even for this 15 yr long simulation, indicating the quality of the analytical estimate. Still, the zonal velocity, u, exhibits larger difference between the numerical and approximated results, since it contains a secular term, [eq. (18)]. In addition, there is practically no meridional wave propagation, indicating that in such planetary scales the assumption of meridional free wave is not so accurate.

The zonal phase speed can be estimated using the so-called Hovmöller (longitude-time) diagram. The slope of wave crests (or troughs) yields the zonal phase speed at the specified latitude. Fig. 5 depicts the longitude-time diagrams (based on meridional velocity v) for latitudes close to the southern edge of the northern segment (Fig. 5a) and close to the northern edge of this segment (Fig. 5b). It is clear that in both latitudes the wave propagates westward approximately with a constant speed and that the zonal phase speed at the southern latitude is much larger than that at the northern wall.

The numerically estimated zonal phase speed at different latitudes is shown in Fig. 5c. It is based on longitude-time diagrams like the ones shown in Figs 5a and b calculated at each latitude. The approximate phase speed given in eq. (21) closely follows the numerical one, where only for latitudes smaller than 30° there is some noticeable difference. The numerical phase speed is computed based on the mean of the first 10 yr of simulations. In contrast, when the same calculation was repeated for the first 1 or 2 yr of simulation only, the difference between the numerical

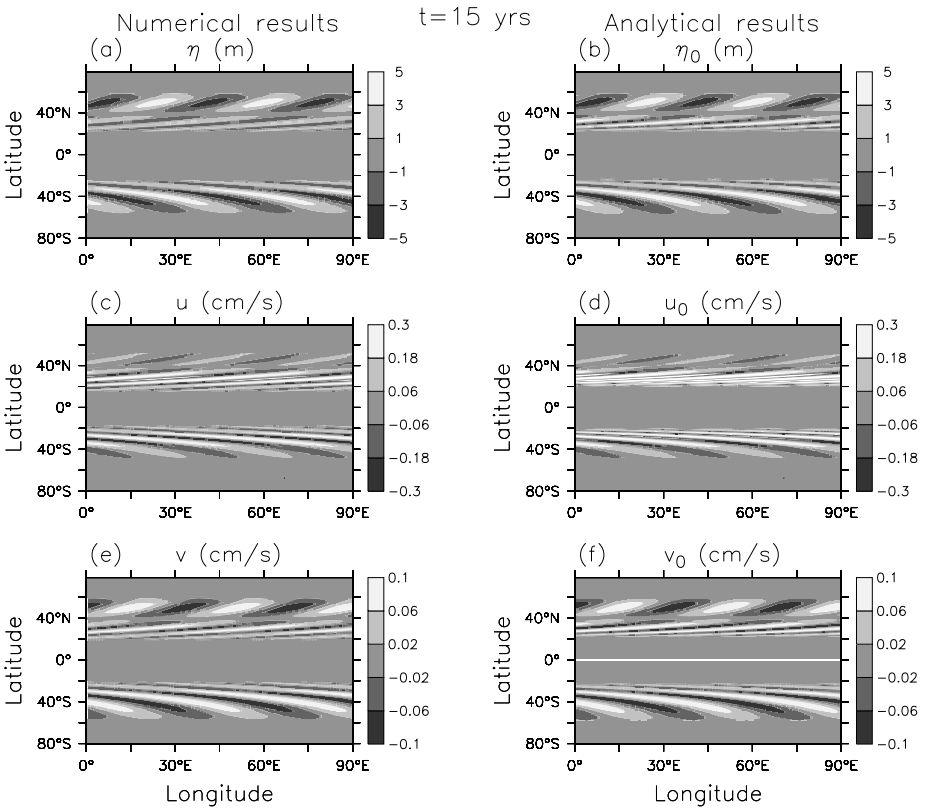

Fig. 4. A comparison between the numerical (left-hand panels) and analytical approximation (right-hand panels) for the free surface η (upper panels), zonal velocity u (middle panels), and meridional velocity v (lower panels). The correspondence between the numerical and analytical approximation results is good. The difference is larger for the zonal velocity as u_0 contains a secular term. Note that only a quarter of the zonal range is shown to allow better visualization.

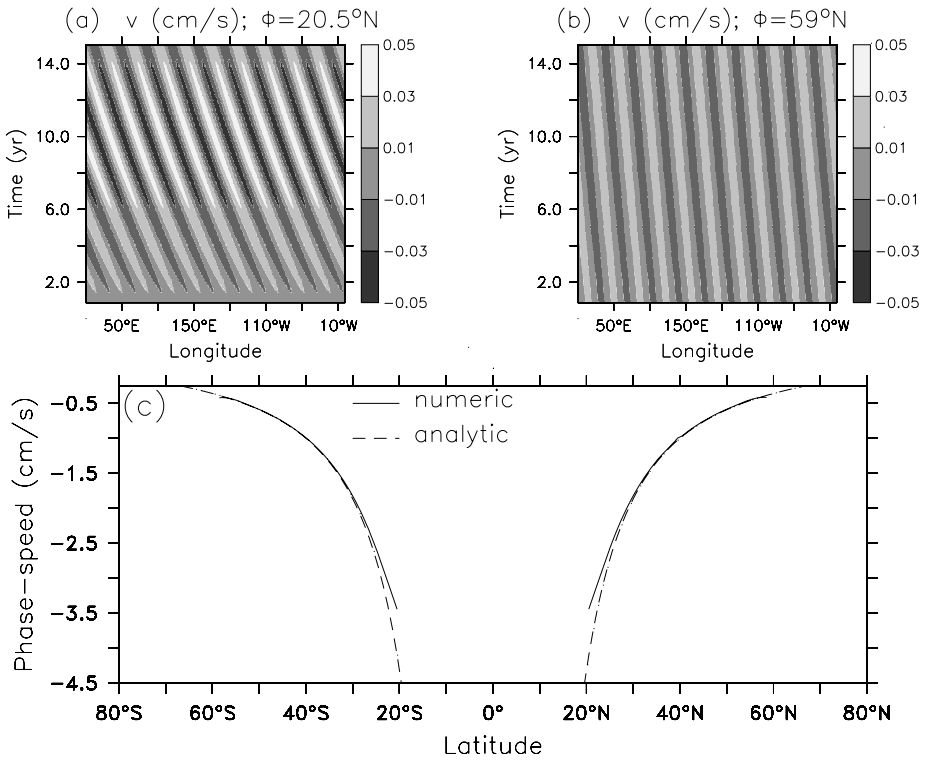

Fig. 5. Longitude-time (Hovmöller) diagrams at a low latitude (a) and high latitude (b) indicating nearly constant wave propagation to the west with a much greater speed at the low latitude. (c) The zonal phase speed as a function of latitude of the numerical simulations (solid) and analytical approximation (dashed) with a good agreement between the two.

and analytical phase speeds is almost indistinguishable everywhere. For longer zonal waves (e.g. $k = 2$ instead of $k = 10$), the agreement between the numerical and analytical results is improved and it remains valid for longer times. This observation is not surprising since $\omega'(\phi)$ increases with the wave number k while the analytical estimate is valid for times $t < 1/\omega'$.

As mentioned above, the total energy of the LSWE is conserved [eq. (20)]. It follows from the nature of the perturbation expansion that the energy of the system should be conserved for each order of approximation as for the zero- and first-order approximations (Appendix A). The total energy of the numerical solution is not conserved, due to the presence of the viscosity terms. Moreover, shorter waves decay faster. Thus, although the time for which the approximation holds is shorter for shorter waves, it might be sufficient, since in reality (and numerical simulations) shorter waves decay faster. In general, it is not expected that a perturbation will persist for more than a few decades, because: (i) viscosity reduces the signal's amplitude and (ii) other perturbations are likely to occur and overcome the imposed perturbation. We conclude, therefore, that from a practical point of view, the time scale over which the suggested approximation is valid, is sufficient to describe natural perturbations, at least for the typical parameter values used here.

We repeated the above numerical experiments starting with different initial conditions, using different wave numbers in the zonal and meridional directions and using initial zonal or meridional velocities instead of the free surface and obtained similar agreement between the numerical calculations and analytical estimates. Simulations without the non-linear advection terms and viscosity terms yielded very similar results with regard to zonal phase speed and wave pattern, so that our numerical results should not be considered as either viscous or non-linear. Moreover, calculations based on the β-plane approximation in a mid latitude channel yielded a phase speed that is very close to the phase speed simulated in the spherical channel and both are very close to the analytical estimate of the zonal phase speeds.

5. Discussion and summary

The best known theory for Rossby waves is based on the quasi-geostrophic approximation. It is, however, known that this theory is valid for meridional scales of up to a few degrees only (the exact figure depends on the Rossby radius of deformation, see, e.g. Poulin, 2009). This known fact is demonstrated numerically in Section 2, using the MITgcm, starting from a quasi-geostrophic eigenmode, for which the numerical simulation exhibited different zonal wave speeds at different latitudes. It was also shown that, starting from the exact eigenmode of planetary Rossby waves on the β-plane (the parabolic cylinder functions), the structure of the wave is preserved in time and a single zonal

phase speed may be associated with each eigenmode. A linear combination of these exact modes yields a wave propagation with latitude-dependent phase speed, since the higher modes whose phase speed is smaller extend farther poleward than the lower modes. The zonal phase speed follows the classical long Rossby waves dispersion relation.

The exact solutions of off-equatorial Rossby waves on the β-plane using the LSWE—parabolic cylinder functions (e.g. Paldor and Sigalov, 2008)—can only be computed numerically to satisfy the boundary conditions. The situation is even more troublesome when dealing with the LSWE on a sphere where an infinite sum of analytical functions (e.g. Longuet-Higgins, 1968b) is needed to construct the exact solution. Such a situation calls for the development of approximate solutions to circumvent the need for summing up an infinite series or resorting to numerical solutions.

We propose a new approximation based on a carefully selected scaling, in which the meridional coordinate appears as a parameter, that is, the underlying differential equation does not contain derivatives with respect to the meridional coordinate. This equation leads to a wave frequency (and hence phase speed) that explicitly depends on latitude (that plays the role of a parameter), where wave propagation is faster towards the equator. In essence, the proposed scaling leads to a long meridional wave approximation. The analytical approximation accounts for arbitrary initial conditions in the meridional direction that satisfy the boundary conditions; the analytical approximation exhibits close similarity with the numerical simulations. The meridional structure of the wave is determined by the initial conditions and there is no need to find the meridional eigenmodes in order to find the time development of the initial perturbation, at least up to some finite times during which the scaling remains valid. The zonal velocity in this approximation contains a secular term that grows with time and, thus, the approximation is valid for times $t < 1/\omega'$ where ω is the wave frequency. The multiple time scale technique is often used to eliminate secular terms in perturbation expansions, by effectively updating the frequency of the lower-order approximation. However, this technique cannot eliminate the secular terms discussed here, because they arise from the explicit dependence of the frequency ω on the meridional coordinate, ϕ, already in the zero-order approximation for u.

The LSWE have only a single small parameter, ε. When applying the scaling of the different variables in the LSWE the outcome is that ε multiplies only the time derivative of the zonal momentum equation, putting the meridional velocity in geostrophic balance. This is a consequence of the different scaling used for the zonal and meridional coordinates. The use of different scaling for the zonal and meridional directions is not new and has been used, for example, in the study of equatorial wave dynamics (e.g. Cane and Sarachik, 1976, 1981; Emile-Geay and Cane, 2009), where the time derivative in the meridional momentum equation is multiplied by the small parameter and hence, to a zero-order approximation, the zonal velocity is in geostrophic balance. Although in this case the corresponding differential equation does contain derivatives with respect to the meridional coordinate, the solution is relatively simple.

The major outcome of the theory proposed in the present study is that the wave frequency is a function of the meridional coordinate. This leads to a secular term in the zonal velocity, through the meridional derivative of the free surface η. Such behaviour is not unique to our theory. The long wave assumption usually leads to planetary geostrophy (e.g. Cessi and Louazel, 2001; Primeau, 2002; Vallis, 2006) and when linearized, the time derivatives in both momentum equations may be neglected (at least to zero order). This leads to a partial differential equation without derivatives with respect to the meridional coordinate, but with the explicit meridional dependence of the Coriolis parameter (e.g. Meyers, 1979; Emile-Geay and Cane, 2009). Thus, as for the approximation suggested here, the wave frequency and zonal phase speed in these studies also depend on latitude and hence the zonal velocity contains a secular term. Yet, the solution obtained by the planetary geostrophic approximation is less general than the one presented above, as more terms are neglected from the LSWE. In addition, we also provide the next order approximation (Appendix A).

The classical quasi-geostrophic Rossby waves zonal phase speed for long planetary waves is (Gill, 1982; Pedlosky, 1987) $C_x \approx -\beta g H / f_0^2$. Our approximation for the phase speed of long Rossby waves in a channel on the β-plane modifies this classical expression, by replacing the Coriolis parameter in the channel centre, f_0, by its local value at latitude y: $f_0 + \beta y$. Moreover, it is possible to reproduce eq. (22) by replacing the β-plane parameters, f_0 and β, with their spherical counterparts $2\Omega \sin\phi$ and $(2\Omega/a)\cos\phi$. However, this correspondence does not mean that the classical Rossby wave theory predicts that a single specific planetary wave will propagate with different speeds at different latitudes. In fact, the present theory bolsters the applicability of the results of the quasi-geostrophic theory regarding the phase speed but without making any assumptions on the meridional variation of the amplitude of the dependent variables, u, v and η.

It is important to highlight the difference between our study and the study of Williams (1985). Williams (1985) basic assumption is geostrophy to a zero-order approximation, meaning that the time derivatives of the shallow water equations (not necessarily linearized) may be neglected at the zero-order approximation. Then, based on this assumption, Williams (1985) developed a general geostrophy (GG) approximation, both on the sphere and the β-plane, that incorporates non-linear advection terms. Then, using various scaling arguments, different approximate equations for the GG equation are proposed; the solution for these equations was not presented by Williams (1985). The zero-order approximation of our study is not the geostrophic balance and in effect only the time derivative of the zonal momentum equation of the LSWE is neglected in the zero-order

approximation; we also provide the zero- and first-order approximated solution.

The standard mathematical set-up for the study of Rossby waves is a channel (e.g. Gill, 1982; Pedlosky, 1987). Obviously, channel-like configurations do not exist on planetary scales. Thus, the channel set-up, required by the traditional mathematical approach was questioned in the past. In the approximation suggested here the 'channel' can be extended from pole–pole (which is quite natural for global scale waves) while an internal basin off-equatorial perturbation may be successfully simulated. This is due to the fact that the meridional coordinate acts like a parameter in the suggested approximation, enabling the use of an arbitrary meridional structure provided only that it satisfies the boundary conditions, which obviously includes internal basin perturbation. We thus conclude that the channel configuration is not a real issue in the theory proposed here.

6. Acknowledgments

We thank Emmanuel Boss, Georgy Burde, Mark Cane, Tom Farrar, Hezi Gildor, Eli Tziperman and Carl Wunsch for helpful comments and discussions. YA thanks the Israel Science Foundation for financial support.

7. Appendix A: Higher-order approximation

The treatment presented below uses non-dimensional variables. It is possible to expand eq. (7) in terms of ε as follows:

$$(\mathfrak{L}_0 + \varepsilon\mathfrak{L}_1 + \varepsilon^2\mathfrak{L}_2)\eta = 0, \tag{A1}$$

where

$$\begin{aligned}
\mathfrak{L}_0 &= \sin^2\phi\cos\phi\left(\sin^2\phi\,\partial_t - \partial_\lambda\right) - \frac{\sin^2\phi}{\cos\phi}\partial_{\lambda\lambda t}\\
\mathfrak{L}_1 &= \sin\phi(\cos^2\phi + 1)\partial_{t\phi} - \cos\phi\sin^2\phi\,\partial_{t\phi\phi} + \cos\phi\,\partial_{tt\lambda}\\
&\quad + 2\cos\phi\sin^2\partial_t^3 - \frac{1}{\cos\phi}\partial_t^3\partial_\lambda^2\\
\mathfrak{L}_2 &= \sin\phi\,\partial_t^3\partial_\phi - \cos\phi\,\partial_t^2\partial_\phi^2 + \cos\phi\,\partial_t^5.
\end{aligned} \tag{A2}$$

Using these operators, the equation for the nth-order approximation in ε is

$$\mathfrak{L}_0\eta_n + \mathfrak{L}_1\eta_{n-1} + \mathfrak{L}_2\eta_{n-2} = 0, \tag{A3}$$

where we set $\eta_{-1} = \eta_{-2} = 0$ such that this equation will also account for the zero- and first-order approximations. The periodic boundary conditions in the zonal direction impose a solution of the form:

$$\eta(\lambda, t, \phi) = e^{\mathrm{i}k\lambda}\bar{\eta}(t, \phi). \tag{A4}$$

Using eq. (A4) and introducing the expression for ω [eq. (12)], $\mathfrak{L}_{0,1,2}$ are found to be all proportional (with the same proportionality coefficient) to:

$$\begin{aligned}
\mathfrak{M}_0 &= \mathrm{i}\omega + \partial_t\\
\mathfrak{M}_1 &= -\frac{\omega}{k}\Big[(2\cot\phi + \tan\phi)\partial_{t\phi} - \partial_{t\phi\phi} + \frac{\mathrm{i}k}{\sin^2\phi}\partial_{tt}\\
&\quad + 2\left(1 + 2k_\lambda^2/\sin^2 2\phi\right)\partial_t^3\Big]\\
\mathfrak{M}_2 &= -\frac{\omega}{k}\frac{\sin\phi\,\partial_t^3\partial_\phi - \partial_t^3\partial_\phi^2 + \partial_t^5}{\sin^2\phi\cos\phi}.
\end{aligned} \tag{A5}$$

The equation for η is $(\mathfrak{M}_0 + \varepsilon\mathfrak{M}_1 + \varepsilon^2\mathfrak{M}_2)\eta = 0$ and the nth-order approximation equation is $\mathfrak{M}_0\eta_n + \mathfrak{M}_1\eta_{n-1} + \mathfrak{M}_2\eta_{n-2} = 0$. Note that $\mathfrak{M}_0$ contains only the first time derivative, a fact that helps in finding the first- (and higher) order approximation. In addition, in these equations, the meridional coordinate acts like a parameter and only a first-order ordinary differential equation has to be solved for each order of approximation.

Using the $\mathfrak{M}_0$ and $\mathfrak{M}_1$ operators it is possible to find the first-order approximation for η using

$$\mathfrak{M}_0\eta_1 + \mathfrak{M}_1\eta_0 = 0, \tag{A6}$$

where $\eta_0 = \bar{\eta}_0(\phi)\exp\mathrm{i}(k\lambda - \omega t) = \bar{\eta}_0(\phi)\exp(\mathrm{i}\theta)$ and $\eta_1 = f_1(t, \phi)\exp(\mathrm{i}k\lambda)$. The aim is to find a particular solution to the above equation. The ϕ derivatives in $\mathfrak{M}_1$ lead to terms that are proportional to t and t^2, as ω is a function of ϕ. The equation to solve is

$$\mathrm{i}\omega\eta_1 + \partial_t\eta_1 + \left(\mathrm{i}a_0 + a_1 t + \mathrm{i}a_2 t^2\right)e^{\mathrm{i}(k\lambda - \omega t)} = 0, \tag{A7}$$

where the coefficients $a_j(\phi)$ are given by:

$$\begin{aligned}
a_0(\phi) &= -\frac{\omega}{k}\left\{-k\csc^2\phi\,\omega^2\bar{\eta}_0 + 2\left(1 + 2k_\lambda^2\csc^2\phi\right)\omega^3\bar{\eta}_0 + 2\omega'\bar{\eta}_0'\right.\\
&\quad + \bar{\eta}_0[\omega'' - (2\cot\phi + \tan\phi)\omega']\\
&\quad \left. + \omega\left[\bar{\eta}_0'' - (2\cot\phi + \tan\phi)\bar{\eta}_0'\right]\right\},
\end{aligned} \tag{A8}$$

$$\begin{aligned}
a_1(\phi) &= -\frac{\omega}{k}\left(2\bar{\eta}_0\omega'^2 + \omega[2\omega'\bar{\eta}_0'\right.\\
&\quad \left. + \bar{\eta}_0(\omega'' - (2\cot\phi + \tan\phi)\omega')]\right),
\end{aligned} \tag{A9}$$

$$a_2(\phi) = \omega^2\omega'^2\bar{\eta}_0/k. \tag{A10}$$

The prime denotes derivative with respect to ϕ. The particular solution to the above equation is

$$\eta_1 = -\left(\mathrm{i}a_0 t + a_1 t^2/2 + \mathrm{i}a_2 t^3/3\right)e^{\mathrm{i}\theta}. \tag{A11}$$

By taking the imaginary (or real) value of η_1 we obtain the real value solution

$$\eta_1 = -a_0 t\cos\theta - \frac{1}{2}a_1 t^2\sin\theta + \frac{1}{3}a_2 t^3\cos\theta. \tag{A12}$$

The first-order approximations for the zonal and meridional velocities u_1 and v_1 may be found using eq. (14).

It is now left to verify whether the first-order approximation solution satisfies the energy preservation given in eq. (20). To a

first order in ε, eq. (20) may be written as:

$$E_1 = \iint \left(u_0^2 + 2v_0v_1 + 2\eta_0\eta_1\right)\cos\,\phi\,\mathrm{d}\,\lambda\,\mathrm{d}\,\phi, \tag{A13}$$

where E_1 stands for the first-order approximation for the total energy of the system. The terms that contain multiplication of $\cos\theta$ and $\sin\theta$ become zero when integrated with respect to λ, due to the periodic boundary conditions in the zonal direction. In addition, terms that are independent of t after the integration are not of interest as they are obviously conserved with time. After excluding these terms and integrating with respect to λ, E_1 becomes

$$E_1 = -\pi t^2 \int_{\phi_1}^{\phi_2} \left[\omega\omega''\bar{\eta}_0 + 2\omega\omega'\bar{\eta}_0' + \omega'^2\bar{\eta}_0 - \omega\omega'(2\cot\phi + \tan\phi)\bar{\eta}_0\right]\frac{\bar{\eta}_0\cos\phi}{\sin^2\phi}\mathrm{d}\phi, \tag{A14}$$

where $\phi_{1,2}$ are the latitudes of the channel walls. It is easy to show that

$$E_1 = -\pi t^2\left[\frac{\omega\omega'\cos\phi\bar{\eta}_0^2}{\sin^2\phi}\right]_{\phi_1}^{\phi_2} = 0, \tag{A15}$$

as $\bar{\eta}_0$ vanishes at the channel walls, $\phi_{1,2}$, since v_0 vanishes at the channel walls and v_0 is proportional to $\bar{\eta}_0$ [eq. (17)].

It is expected that the energy of the system will be conserved for each order of approximation in ε, even in the presence of secular terms.

References

Adcroft, A., Campin, J.-M., Heimbach, P., Hill, C. and Marshall, J. 2002. MITgcm release manual (online documentation), MIT/EAPS, Cambridge, MA 02139, USA. http://mitgcm.org/sealion/online_documents/manual.html.

Cane, M. A. and Sarachik, E. S. 1976. Forced baroclinic ocean motions I: the linear equatorial unbounded case. *J. Mar. Res.* **34**, 629–664.

Cane, M. A. and Sarachik, E. S. 1981. The response of a linear baroclinic equatorial ocean to periodic forcing. *J. Mar. Res.* **39**, 651–693.

Cessi, P. and Louazel, S. 2001. Decadal oceanic response to stochastic wind forcing. *J. Phys. Oceanogr.* **31**, 3020–3029.

Chelton, D. B., deSzoeke, R. A., Schlax, M. G., El-Nagger, K. and Siwertz, N. 1998. Geophysical variability of the first baroclinic Rossby radius of deformation. *J. Phys. Oceanogr.* **28**, 433–460.

De-Leon, Y. and Paldor, N. 2011. Zonally propagating wave solutions of Laplace Tidal Equations in a baroclinic ocean of an aqua-planet. *Tellus A* **63A**, 348–353.

Emile-Geay, J. and Cane, M. A. 2009. Pacific decadal variability in the view of linear equatorial wave theory. *J. Phys. Oceanogr.* **39**, 203–219.

Gill, A. E. 1982. *Atmosphere–Ocean Dynamics Gill*, A. E. Academic Press, London.

Hough, S. S. 1898. On the application of harmonic analysis to the dynamical theory of the tides. II. On the general integration of Laplace's tidal equations. *Philos. Trans. Roy. Soc. Lond. A* **191**, 139–185.

LeBlond, P. H. and Mysak, L. A. 1978. *Waves in the Ocean*. Elsevier Oceanography Series. Elsevier, Amsterdam.

Longuet-Higgins, M. S. 1968a. Double Kelvin waves with continuous depth profiles.. *J. Fluid Mech.* **34**, 49–80.

Longuet-Higgins, M. S. 1968b. The eigenfunctions of Laplace's tidal equations over a sphere. *Philos. Trans. Roy. Soc. Lond. A* **262**(1132), 511–607.

Margules, M. 1893. Luftbewegungen in einer rotierenden sphiroidschale. *Sber. Akad. Wiss. Wien* **102**, 11–56.

Marshall, J., Adcroft, A., Hill, C., Perelman, L. and Heisey, C. 1997a. A finite-volume, incompressible Navier Stokes model for studies of the ocean on parallel computers. *J. Geophys. Res.* **102**C3, 5753–5766.

Marshall, J., Hill, C., Perelman, L. and Adcroft, A. 1997b. Hydrostatic, quasi-hydrostatic, and nonhydrostatic ocean modeling. *J. Geophys. Res.* **102**(C3), 5733–5752.

Meyers, G. 1979. On the annual Rossby wave in the tropical North Pacific ocean. *J. Phys. Oceanogr.* **9**, 663–674.

Paldor, N. and Sigalov, A. 2008. Trapped waves on the mid-latitude beta-plane. *Tellus* **60A**, 742–748.

Pedlosky, J. 1987. *Geophysical Fluid Dynamics*. 2 Edition. Springer-Verlag, Berlin-Heidelberg-New York.

Pedlosky, J. 2003. *Waves in the Ocean and Atmosphere.* Springer-Verlag, Berlin-Heidelberg-New York.

Poulin, F. J. 2009. Can long meridional length scales yield faster Rossby waves? *J. Phys. Oceanogr.* **39**(2), 472–478.

Primeau, F. 2002. Long Rossby wave basin-crossing time and the resonance of low-frequency basin modes. *J. Phys. Oceanogr.* **32**, 2652–2665.

Rossby, C. G. 1939. Relation between variation in the intensity of the zonal circulation of the atmosphere and the displacement of the semi-permanent centers of action. *J. Mar. Res.* **2**(1), 38–55.

Schopf, P. S., Anderson, D. L. T. and Smith, R. 1981. Beta dispersion of low-frequency Rossby waves. *Dyn. Atmos. Oceans* **5**, 187–214.

Vallis, G. K. 2006. *Atmospheric and Oceanic Fluid Dynamics.* Cambridge University Press, Cambridge, UK.

Williams, G. P. 1985. Geostrophic regimes on a sphere and a beta plane. *J. Atmos. Sci.* **42**(12), 1237–1243.